Measurement of fluid velocity fields using digital correlation techniques

Donald R. Matthys
Marquette University, Physics Department
Milwaukee, WI 53233

John A. Gilbert
University of Alabama in Huntsville, Dept. of Mechanical Engineering,
Huntsville, AL 35899

Joseph T. Puliparambil
Marquette University, Dept. of Electrical Engineering
Milwaukee, WI 53233

ABSTRACT

Digital correlation is basically a pattern matching procedure. Two images of a seeded fluid are taken and the intensity distribution of a small window in the first image is matched in the second image using statistical correlation methods. A technique for enhancing the apparent seeding density of the fluid by combining an aperiodic sequence of images is described, which is similar in concept to the multiple exposure technique of the Young's fringes method of analysis, but which must be carefully applied.

1. INTRODUCTION

Full-field laser velocimetry has recently developed into a powerful experimental technique for flow visualization. In most cases, a transparent fluid is seeded with particles or tracers which are carefully chosen to ensure that their movement accurately follows the flow. The movement of these particles is observed in a reference plane which is usually illuminated using a single collimated beam of coherent laser light conveniently shaped into a thin sheet and passed through the fluid volume. If the seeding concentration is low, such that the particle images are discrete and rarely overlap in the image plane, there is little or no interference and the coherent properties of the illumination are largely irrelevant. In this so-called "particle image mode",[1] an image pattern is derived from light scattered by the moving field of seed particles, and velocity information may be obtained by analyzing different image patterns recorded using appropriately timed exposures. The scatterers must be large enough and numerous enough to provide a strong signal, yet small and neutrally buoyant to ensure that they follow the flow, and must be of a sufficiently low concentration to avoid altering the flow characteristics or excessively increasing the opacity of the fluid.[2]

The first successful demonstrations of laser speckle velocimetry (LSV) were reported for Poiseuille flow (simple unidirectional laminar flow in a long circular pipe)[3,4,5] and relied on the laser speckle mode and the Young's fringes method of analysis. This approach was later applied to study the more complicated two-dimensional flow encountered in Rayleigh-Benard convection (a layer of fluid cooled on top and/or heated from below).[6]

In other two-dimensional flow studies, where a lower seeding density was employed, investigators used the particle image mode and recorded multiple exposures of individually imaged particles to enhance the contrast of Young's fringes.[7,8] Optical Fourier filtering techniques were also employed in these studies to generate velocity component fields. More recently, a detailed study of Rayleigh-Benard convection was reported which used the mechanically chopped illumination from a relatively low power (5 mW) laser.[9] In this study, multiple exposure

specklegrams were analyzed using both full-field Fourier filtering methods and hybrid Young's fringes techniques. Semi-automated methods were applied to obtain velocity, vorticity, and streamline maps.

Traditional procedures for analyzing specklegrams are mainly divided into two approaches: methods that use pointwise interrogation to obtain Young's fringes and methods that utilize fringes resulting from optical filtering. Although significant strides have been made to improve and automate these approaches, each has its own limitations.

The Young's fringes technique can give the direction and magnitude of flow, but with an ambiguity in the sign of the flow direction. Although special means can be utilized to resolve the sign ambiguity,[10,11,12] a more basic problem is that the technique cannot measure displacements smaller than the diameter of the microparticles seeded in the fluid, and if the particles are very small the intensity of the scattered light becomes weak. Also, the need for laser light to interrogate the specklegram containing the image data introduces secondary speckle into the Young's fringes being measured, and limits the accuracy with which their positions can be determined.

The method of Fourier filtering, on the other hand, gives a full field measurement immediately, but only of a particular component of the velocity vector. To obtain more information about the fluid flow, a velocity selecting aperture must be moved radially and tangentially around the center of the diffraction halo produced by the speckle pattern being studied. The need for laser illumination introduces secondary speckle which, if the aperture is kept small to select a narrow frequency range, makes the fringes in the filtered image difficult to read.

An alternative method that employs photo-electronic techniques to digitize successive particle image patterns for subsequent numerical correlation was introduced a few years ago.[13] This qualitatively successful pioneering application of wholly digital processing to an evaluation of Poiseuille flow completely eliminated the need to photographically record and optically correlate speckle data. However, this early work used a VAX computer to perform the correlations between two images, required a relatively large 2-watt argon ion laser to illuminate the moving fluid, and was performed with a heavily seeded mixture of 50-percent glycerine/50-percent water by volume. Similar approaches to fluid visualization have been tried using machine vision systems. One approach, for example, relied on digitizing successive images recorded at equally spaced time intervals.[14] In this case, the motion of the mass centers of the particles in a lightly seeded fluid were tracked using a desk-top computer but the technique could only be applied in a semi-automated mode of operation.

The current work expands on the approach of digital correlation and introduces a new aperiodic recording technique which utilizes a low powered He-Ne laser (10 mW), a desk-top computer, and a lightly seeded fluid. As opposed to optical methods, this technique does not need to use laser light to interrogate the image pattern, so no secondary speckle is introduced. Also, the lower limit of displacement measurement is determined by the resolution of the sensor used and the magnification of the camera, and can be much lower than the speckle size, so a considerably wider range of measurement is possible than can be attained by optical processing. The technique can be completely automated; since no mechanical scanning of the image is required, the technique is potentially much faster than all of the optical methods currently used for flow visualization.

2. VELOCITY MEASUREMENT BY DIGITAL CORRELATION

Digital correlation is a method of pattern recognition in which a small subset of an initial image is located in a second (deformed or displaced) image.[15] A standard equation found in many textbooks which is generally used to determine the correlation coefficient, ρ, for a data window taken from the first image and centered over location (m,n) in the displaced image is[16]

$$\rho(m,n) = \frac{\Sigma_x\Sigma_y[f(x,y) - \langle f\rangle][w(w-m,y-n) - \langle w\rangle]}{\{\Sigma_x\Sigma_y[f(x,y) - \langle f\rangle]^2\ \Sigma_x\Sigma_y[w(x-m,y-n) - \langle w\rangle]^2\}^{1/2}} \quad (1)$$

where f(x,y) are the intensity values of the second image for those locations under the window values w(x,y) as the window is moved over a suitably chosen search range (x,y), <f> is the average intensity value of the region located under the window, and <w> is the average intensity value of the window. The maximum correlation value indicates the best match of the chosen subset from the initial image as located in the second image. It should be pointed out that there is some question as to the validity of using ρ to measure correlation strength in two-dimensional images.[17] When ρ is defined by the formula given above it is known as the Pearson coefficient, and a linear relationship is assumed to exist between the two sets of data being compared. Statistic textbooks[18] frequently give examples showing data sets that have a very low correlation value, ρ , but which are nevertheless very strongly correlated. The cause of the low value of ρ for these textbook examples is usually that the relation between the data sets is non-linear. In addition to this problem, another difficulty with applying correlation methods to image patterns is that the underlying distribution of the numbers being compared under the correlation window is unknown. The usual criterion for justifying the use of the Pearson coefficient is that the distribution of data values from the two sets should jointly form a binormal distribution around their average values. Because of these restrictions, another approach to using correlation for pattern matching which uses a rank-ordering technique, is sometimes proposed, in which the sets of data values being compared under the window are replaced with their rank order within the set. The statistic is then called the Spearman coefficient, and the formula used is identical to the one given earlier, except for the replacement of the original data intensity values by rank order, both for the window and for the region underneath it. In this approach, the underlying distribution is perfectly known and there is no question about the validity of applying the correlation method.

A final problem with the correlation approach is that the procedure will always return some location as having the highest correlation value. Even if the window region being matched has very little content, i.e., no large particle images and only noise fluctuations present, a similarly empty region in the second image will be specified as having the best match, sometimes with a surprisingly high correlation value. To obviate this problem, a "structure function" is used to ensure that the window being matched has enough content in terms of the number of particle images with different intensities and relative orientations to reject such spurious matches. During the selection of windows to be matched, if a particular window lacks structure, it will be rejected and a new window will be have to be chosen that meets the requirements of the structure function being used.

3. DEVELOPMENT OF THE METHOD: SIMULATED DATA

A uniform flow field was simulated to test computer algorithms for digital correlation and to carefully study different approaches for recording, combining, and correlating digitized image pairs. This was accomplished by mounting a black card splattered with white paint on a translation stage. Sixteen data files were recorded of the simulated scatterers as the card was translated horizontally from left to right through equal increments of 0.0635 cm (0.025") for a total of 0.952 cm (0.375"); the horizontal calibration factor was 0.0047 cm/column (0.00185"/column). Images were captured using a Matrox image processing board and were saved as 256x256 digital arrays of 8 bit numbers with intensity values ranging from 0 to 255. Figure 1, for example, shows an image of the simulated scatterers in their original locations. Pixel coordinates were measured from an origin located in the upper left hand corner of the computer screen with x (columns) positive to the right, and y (rows) as positive down. The sixteen files were called "file1" through "file16".

The basic approach described in Reference 13 was applied at several points in file1 to compute the displacement which occurred between the time in which file1 and file2 were recorded. Theoretically, the displacement of all

points should be equal, since the card translates as a rigid body. This operation was carried out by selecting a 15 pixel square window centered around each point selected in file1. This window was compared to windows of equal dimensions contained in file2 and centered over pixels included within a user-specified search region. Each comparison produces a correlation coefficient; the displaced location of the window selected from file1 is assumed to occur at the pixel location in file2 where the correlation coefficient attains a maximum value. Since it was known *a priori* that the test card was translated from left to right, correlation coefficients were computed over a limited search range, extending horizontally from 0 to 40 pixels, and vertically from minus to plus 20 pixels, measured relative to the pixel location of the point chosen in file1.

Figure 1. Image of simulated scatterers obtained by splattering a black card with white paint.

Figure 2 shows the relatively complex intensity distribution corresponding to three scatterers contained within a window centered at pixel location (75,184). Correlations performed using this window produce a distinct correlation peak, located approximately 13 columns (0.061 cm or 0.024") to the right of the point in question. These results are depicted in Figure 3, where the correlation values are plotted as contours, with the outer contour having a value of 0.4 and each succeeding interior ring representing an increment in ρ of 0.1. The maximum correlation value is relatively high at approximately 0.9.

Figure 4, on the other hand, illustrates that the window centered at pixel coordinates (128,128) contains a single scatterer and, as shown in Figure 5, several large peaks are observed when correlation coefficients are evaluated over the search region. Although the largest peak occurs at the displaced position, approximately 13 columns (0.061 cm or 0.024") to the right of its initial location of the point in question, the lack of structure in the window would most likely present a problem in a real fluid, where the intensity of particles fluctuates as a function of time/position. In this case, one of the other peaks may dominate, resulting in a false prediction of the displacement/velocity.

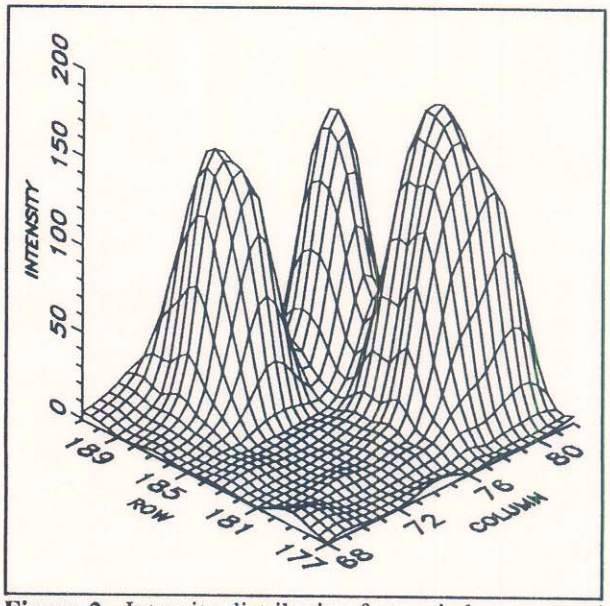

Figure 2. Intensity distribution for a window centered at pixel location (75,184) in a single digitized image of the test card.

One approach to solving this problem is to effectively increase the number of scatterers in the field by combining several images. This was accomplished by a computer algorithm which compared, on a pixel-by-pixel basis, the intensity values in all files to be combined; the largest value at each pixel location was retained in the combination. The algorithm was used to form two sets of five files each, starting with ten separate files (file1, file2, ..., file10) as follows: file1, file3, file5, file7, file9 were combined into the first set, and file2, file4, file6, file8, file10 were combined into

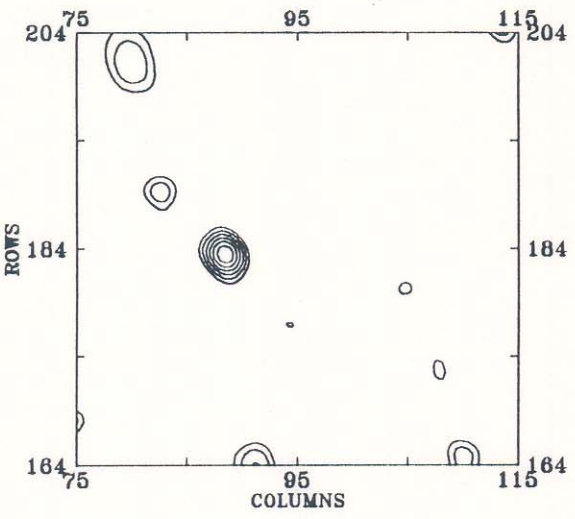

Figure 3. Correlation values over the search region for the window shown in Figure 2. The outer contour has a correlation value ρ of 0.4 and each successive interior ring represents an increment in ρ of 0.1.

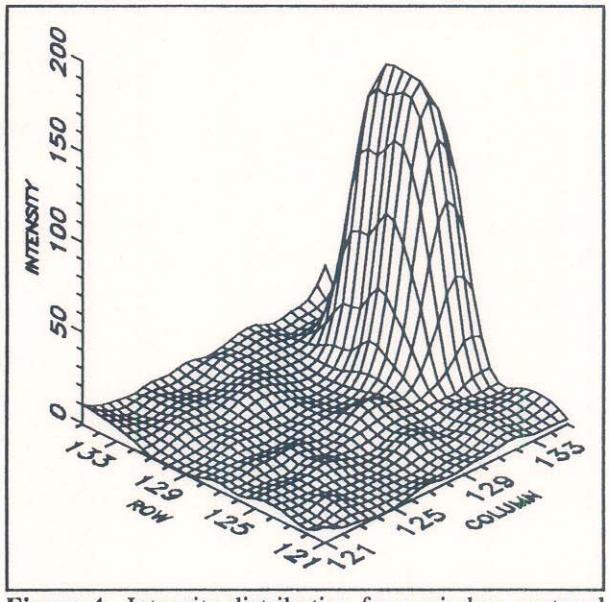

Figure 4. Intensity distribution for a window centered at pixel location (128,128) in a single digitized image of simulated data.

the second. For the purpose of discussion, these combinations are called **initial** and **final**, respectively.

Figure 6 shows the image digitally stored as the file called **initial**. The increase in the number of scatterers is obvious when this figure is compared to Figure 1. As shown in Figure 7, the window at (128,128) is now highly

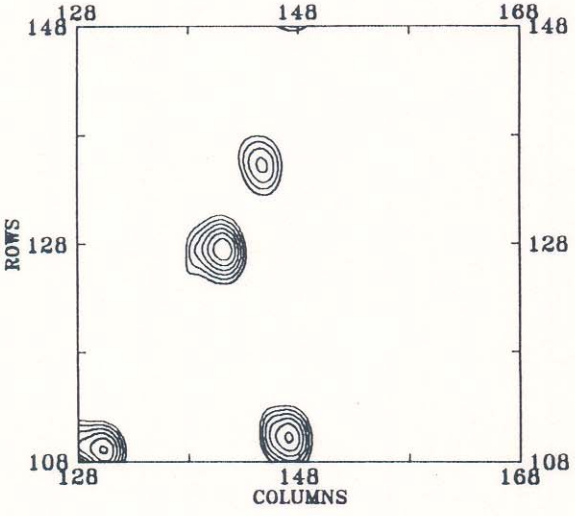

Figure 5. Correlation values over the search region for the window shown in Figure 4.

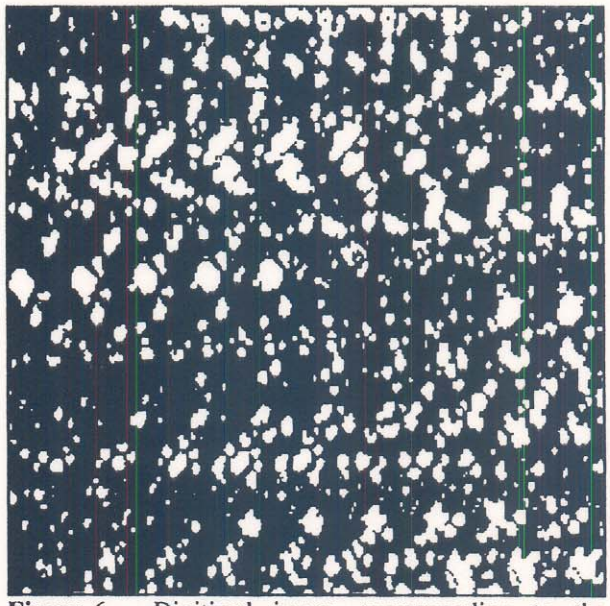

Figure 6. Digitized image corresponding to the superposition of five different recordings.

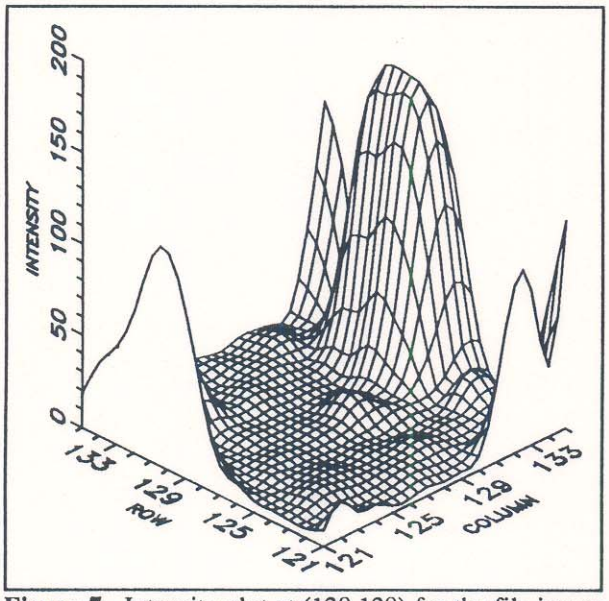

Figure 7. Intensity plot at (128,128) for the file image shown in Figure 6.

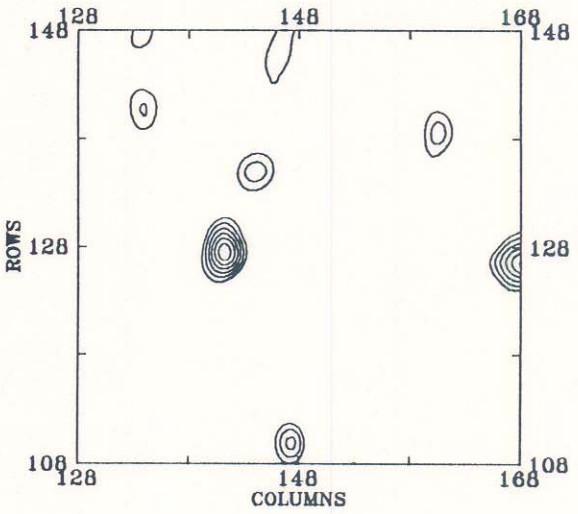

Figure 8. Correlation values over the search region for the point shown in Figure 7.

structured. However, as shown in Figure 8, two distinct peaks of nearly equal amplitude are observed in the search region. This can be attributed to the periodicity of the data. Moreover, other peaks are observed when the search range is expanded. The distance to the first peak is equal to the actual displacement, with subsequent peaks spaced at twice that distance.

Figures 9-12 have been included to understand why these peaks occur. Figure 9 shows three scatterers as they move across the field of view to the right; each of the eight rectangular boxes represents a separate recording. Pairs of files are taken at a constant time interval Δt apart with an arbitrary time interval Δi between the final recording of one image pair and the initial recording of the next image pair. Although other scatterers might move into the field of view they have been omitted for the sake of clarity. Figure 10 depicts the initial and final files as they would appear if they were combined by the algorithm discussed above. As indicated in the figure, a window selected from the initial file matches a window in displaced file when

$$t = \Delta t + (n-1)\Delta i \qquad (2)$$

The location of the peaks observed in the correlation map for the simulated data shown in Figure 8 are verified when Equation 2 is applied with $\Delta t = \Delta i$. Computer programs could be written to search for these multiple peaks so that displacement/velocity could be measured, however, there may be a better alternative; namely, aperiodic recording.

This approach is schematically illustrated in Figure 11 and Figure 12. In this case, Δt is kept constant while Δi is randomly varied. This results in a unique match when the files are combined and correlated.

The approach was applied to the simulated data by combining 10 files into two sets of five, with each pair separated by unequal increments as follows: **initial** consisted of file1, file3, file6, file10, file15; and **final** consisted of file2, file4, file7, file11, file16. Figure 13 shows the correlation map over the search region for the point located at (128,128) with a pronounced peak at the expected location.

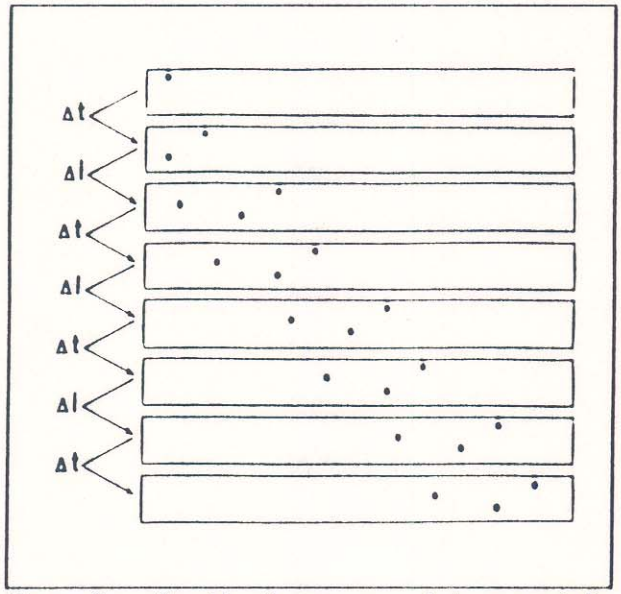

Figure 9. Speckle images recorded at periodic intervals.

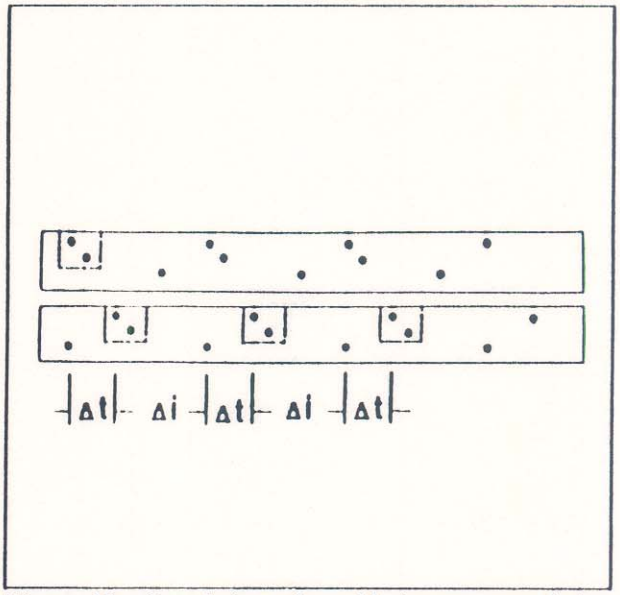

Figure 10. Correlation of speckle images recorded at periodic intervals.

A large search region was then inspected for the two cases of multiple file combination, periodic and aperiodic. The results are shown in Figure 14 and Figure 15, respectively. This shows the success of the theory expressed in Equation 2, but there are still some precautions that must be taken. Although this approach of combining files was successful for the window at (128,128) as shown by the single correlation peak in Figure 13, nevertheless, because of the relatively low particle density, the approach of simply combining files cannot guarantee that all windows chosen over a relatively large field of view will be sufficiently structured to produce a valid

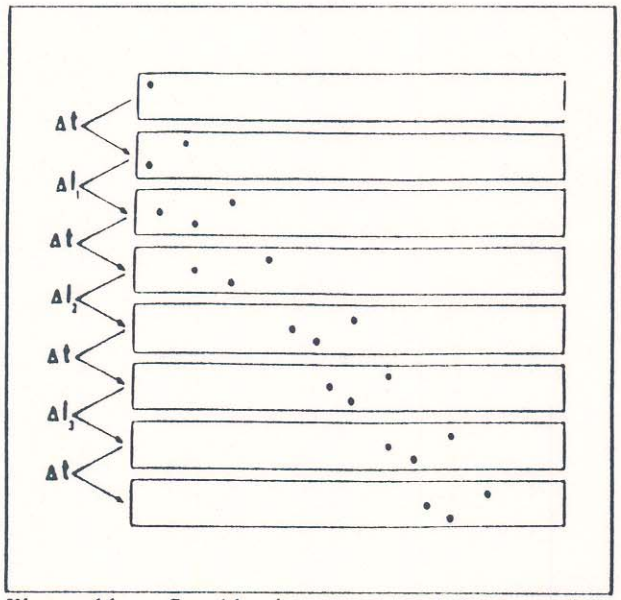

Figure 11. Speckle images recorded at random intervals.

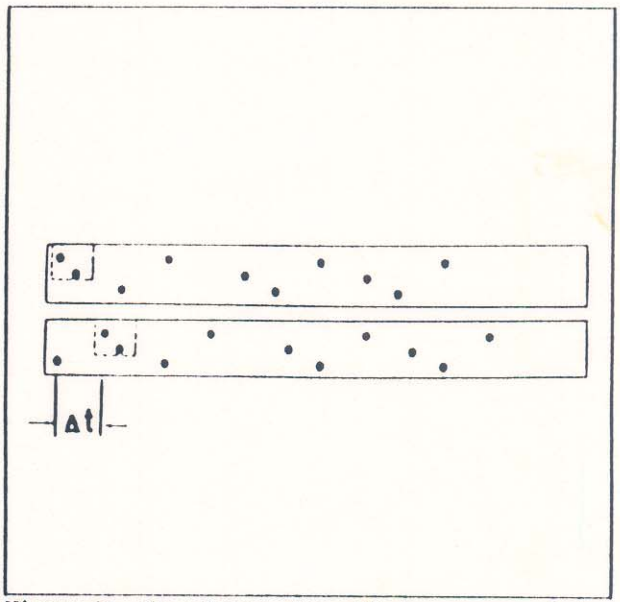

Figure 12. Correlation of speckle images recorded at random intervals.

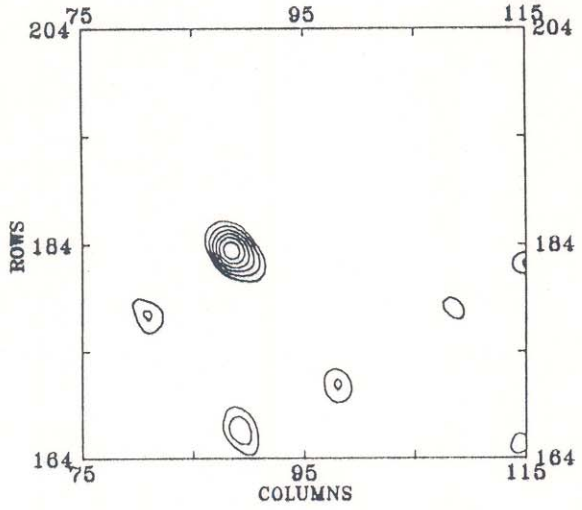

Figure 13. Correlation map obtained for aperiodic recording of simulated data. Outer contour represents correlation value of 0.4, with each inner ring corresponding to an increment of 0.05.

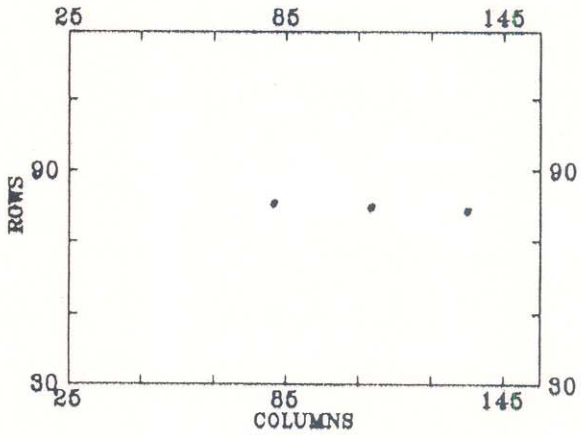

Figure 14. Search over large region of combined files of simulated data with uniform time Δi between files. Multiple peaks of high correlation ($\rho \geq 0.86$) occur along direction of flow.

measurement. A structure function must be defined and applied to each window to make sure that the window does indeed contain enough particles to produce good results.

4. APPLICATION OF THE METHOD: REAL DATA

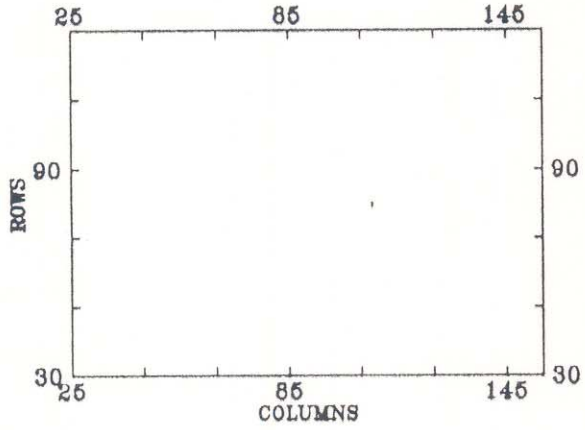

Figure 15. Result of search over large region of combined files of simulated data with random times Δi between files. There is a single peak with $\rho = 0.86$.

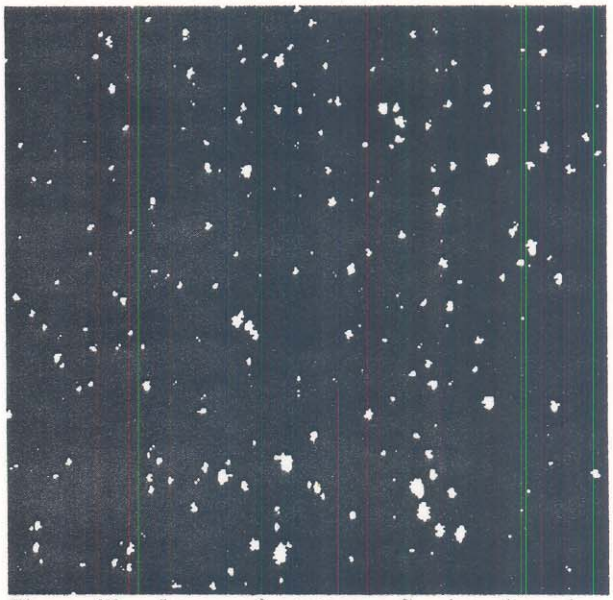

Figure 16. Image of scatterers flowing through a rectangular test cell.

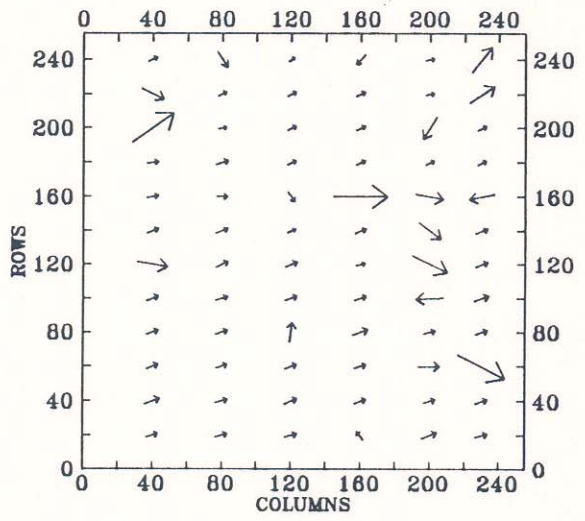

Figure 17. Velocity measurements over a large field of view for a single file of real data. No structure function was used so erroneous results appear.

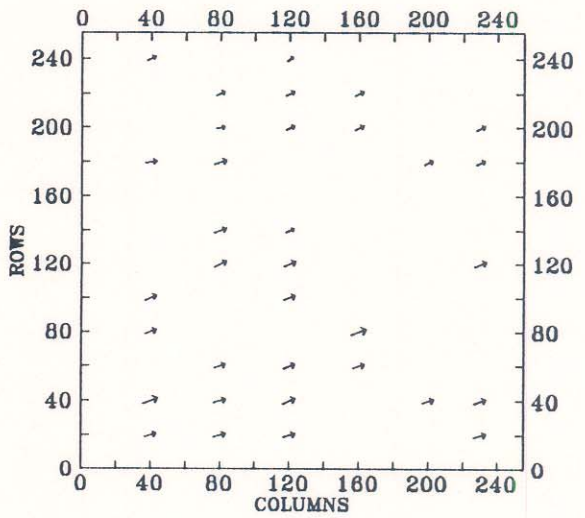

Figure 18. Velocity measurements over a large field of view for a single file of real data. A structure function was used.

To obtain real data, a 30.5 cm (12") cell with a 1.27 (0.5") square cross section was used to obtain a relatively linear flow of water that had been lightly seeded with 15 micron diameter plastic spheres. Images, such as the one shown in Figure 16, were digitized over a 1.5 cm (0.6") long section near the middle of the cell; fluid

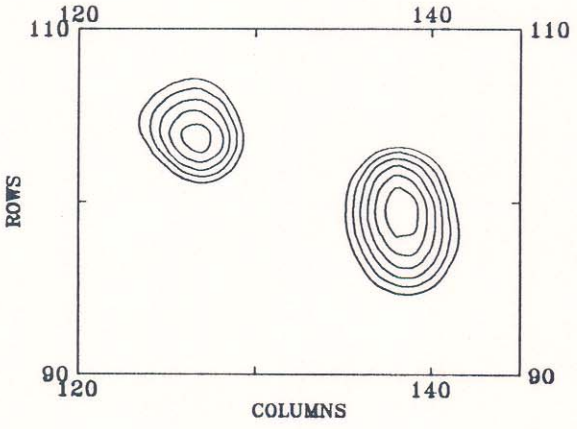

Figure 19. Correlation contours obtained using the Pearson method of correlating intensity values. The outer contour represents a value of 0.4 and each succeeding ring corresponds to an increment of 0.1.

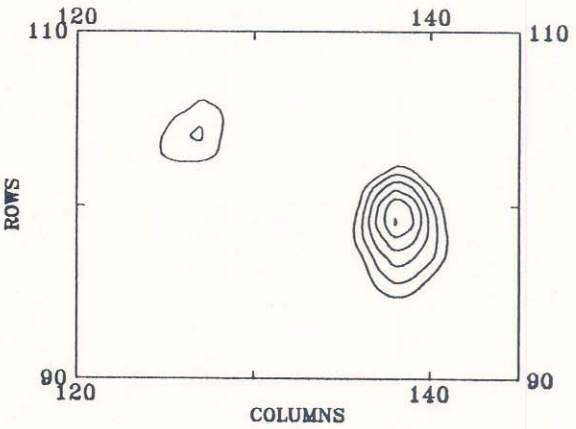

Figure 20. Correlation contours obtained using the Spearman method of correlating the rank order of the intensity values.

	X	Y	dX	dY	ρ
1	40	60	5.0	-1.8	0.958
2	40	140	5.0	-2.0	0.739
3	80	140	4.0	-1.0	0.897
4	80	180	5.0	-2.0	0.909
5	120	160	4.0	-2.0	0.867

Table I. Set of displacements obtained using Pearson correlation method.

	X	Y	dX	dY	ρ
1	40	60	5.0	-1.8	0.958
2	40	140	5.0	-2.0	0.506
3	80	140	4.0	-1.0	0.647
4	80	180	5.0	-2.0	0.781
5	120	160	4.0	-2.0	0.620

Table II. Set of displacements obtained using Spearman correlation method.

velocity was approximately 1 cm/s (0.394 in/s). The method of file combination and structure function was applied to images obtained from the fluid flow and the results are shown in Figure 17 and in Figure 18. Figure 17 shows the result of specifying windows over a 6x12 grid covering the entire field of view when no structure function was used. Some of the windows were basically empty and the resulting velocity measurements contained numerous false values. On the other hand, Figure 18 shows that when a structure function was employed which required that each window have enough bright pixels to guarantee two particle images, the false readings were eliminated. However, the searching algorithm which moved the window from its original grid position to a neighboring location where particles were detected produced a non-uniform grid of measurements.

The next test performed was to determine whether the choice of the Pearson intensity value correlation or the Spearman rank-ordered correlation was important. Tables 1 and 2 show the displacement values obtained by using each of the two methods. The two Tables show that the same displacement values were obtained, though the actual value of the correlation coefficient was generally lower for the Spearman method. Figure 19 and Figure 20 show contour plots of the correlation values obtained by each method, and indicate that the curves are "close enough" to a binormal distribution to justify using the Pearson method. Since the Spearman method is much slower, due to the need for sorting the data each time a window is moved, while producing similar results as the Pearson technique, all later work was done using the Pearson technique.

A slightly different approach was taken for recording aperiodic real data. A total of eight file pairs were

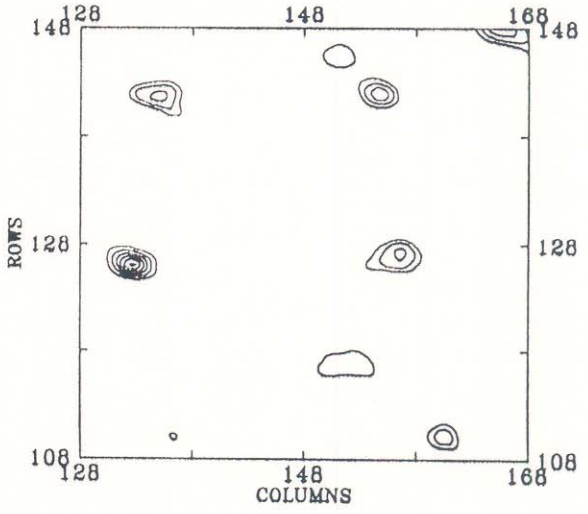

Figure 21. Correlation map obtained by aperiodic recording for a point located at (128,128). Outer ring represents a correlation of 0.4, with each inner ring corresponding to an increment of 0.1.

recorded with the initial and final recordings separated by a constant Δt equal to 33 ms; however, the interval Δi was randomly varied after each pair was recorded. The resulting correlation windows were highly structured and, as shown in Figure 21, a typical correlation map over the search region displayed a distinct peak. In general, peak correlation values were lower than those obtained for the simulated data.

5. CONCLUSIONS

A novel method of correlating a series of image pairs so as to obtain the effect of heavy seeding from what is actually a light seeding was developed and validated by first testing the method on a set of images of simulated data and then by measuring the actual flow in a test cell filled with water that had been seeded with 15-micron spheres. This ability to use a time series of images means that the investigator can work with images selected from the whole set to obtain more detailed information in regions of particularly high or low velocity; also, if the images were stored on film, it is possible to magnify selected regions of interest for high resolution analysis, down to the resolution of the film and camera system.

Since correlation depends on randomness in the data, it might be thought that collating sets of image pairs for analysis would introduce a patterned structure into the image and lead to spurious results, but by using aperiodic time intervals between image pairs, any periodicity can be eliminated. The results of experimental tests are excellent and indicate that the digital correlation technique may have significant advantages over optical processing methods in the range of velocity measurements possible and the speed and accuracy with which results can be obtained.

6. ACKNOWLEDGEMENTS

This work was supported by the George C. Marshall Space Flight Center, National Aeronautics and Space Administration, under co-operative agreement NCC8-15. The authors would like to extend special thanks to Rudy Ruff for his interest in and support of this research.

7. REFERENCES

1. Adrian, R.J., "Scattering particle characteristics and their effects on pulsed laser measurements of fluid flow: speckle velocimetry vs. particle image velocimetry," Applied Optics, 23(11): 1690-1691 (1984).

2. Adrian, R.J., Yao, C.S., "Pulsed laser technique application to liquid and gaseous flows and the scattering power of seed materials," Applied Optics, 24(1): 44-52 (1985).

3. Grousson, R., Mallick, S., "Study of the flow pattern in a fluid by scattered laser light," Applied Optics, 16(9): 2334-2336 (1977).

4. Barker, D.B., Fourney, M.E., "Measuring fluid velocities with speckle patterns," Optics Letters, 1(4): 135-137 (1977).

5. Dudderar, T.D., Simpkins, P.G., "Laser speckle photography in a fluid medium," Nature, 270(5632): 45-47 (1977).

6. Simpkins, P.G., Dudderar, T.D., "Laser speckle measurements of transient Benard convection," Journal of Fluid Mechanics, 89(4): 665-671 (1978).

7. Iwata, K., Hakoshima, T., Nagata, R., "Measurement of flow velocity distribution by multiple exposure speckle photography," Optics Communications, 25(3): 311-314 (1978).

8. Meynart, R., "Equal velocity fringes in Rayleigh-Benard flow by a speckle method," Applied Optics, 19(9): 1385-1386 (1980). By the same author see also "Flow velocity measurement by a speckle method," Proc. of the 2nd European Congress on Optics Applied to Metrology, SPIE Vol. 210, pp. 25-28 (1979).

9. Arroyo, M.P., Yonte, T., Quintanilla, M., Saviron, J.M., "Velocity measurements in convective flows by particle image velocimetry using a low power laser," Optical Engineering, 27(8): 641-649 (1988).

10. Marko, K.A., Rimai, L., "Video recording and quantitative analysis of seed particle track images in unsteady flows," Applied Optics, 24(21): 3666-3672 (1985).

11. Adrian, R.J., "Image shifting technique to resolve directional ambiguity in double-pulsed velocimetry," Applied Optics, 25(21): 3855-3858 (1986).

12. Coupland, J.M., Pickering, C.J.D., Halliwell, N.A., "Particle image velocimetry: theory of directional ambiguity removal using holographic image separation," Applied Optics, 26(9): 1576-1578 (1987).

13. He, Z.H., Sutton, M.A., Ranson, W.F., Peters, W.H., "Two-dimensional fluid-velocity measurements by use of digital-speckle correlation techniques," Experimental Mechanics, 24(2): 117-121 (1984).

14. Batur, C., Braun, M.J., "Flow measurement with non-intrusive machine vision," Proc. of the ISA '88, International Conference and Exhibit, Houston, Texas, October 16-21, 1988, pp. 261-266.

15. Chu, T.C., Ranson, W.F., Sutton, M.A., Peters, W.H., "Applications of digital-image-correlation techniques to experimental mechanics," Experimental Mechanics 25, 232-244 (1985).

16. Gonzalez, R.C., Wintz, P., *Digital Image Processing*, 2nd edition, Addison-Wesley, 1987, p. 426.

17. Press, W.H., *Numerical Recipes in C*, Cambridge Press, 198, page 503.

18. Freedman, Pisani, and Purves, *Statistics*, W.W. Norton, Inc., New York, 1978, page 124.